

# Pairing of a trapped resonantly-interacting fermion mixture with unequal spin populations

Masudul Haque and H. T. C. Stoof  
 Institute for Theoretical Physics, Utrecht University,  
 Leuvenlaan 4, 3584 CE Utrecht, the Netherlands  
 (dated: March 23, 2004)

We consider the phase separation of a trapped atomic mixture of fermions with unequal spin populations near a Feshbach resonance. In particular, we determine the density profile of the two spin states and compare with the recent experiments of Partridge et al. [4]. Overall we find quite good agreement. We identify the remaining discrepancies and pose them as open problems.

**Introduction** | The usual Bardeen-Cooper-Schrieffer (BCS) theory of Bose-Einstein condensation (BEC) of fermion pairs requires the populations of the two species involved in the  $s$ -wave pairing to be equal. For a long time, therefore, theorists have discussed fermionic pairing when the species densities are unequal, and several proposals for the ground state have been put forward [1, 2, 3]. Experimentally, however, such superfluid states with unequal densities have remained elusive.

After several years of experimental studies of the BEC-BCS crossover with equal spin population, experiments with ultracold atoms have very recently also turned to studying superfluidity with unequal populations [4, 5]. The basic idea is to load a trap with an unequal population of two hyperfine states of  $^6\text{Li}$  and tune the bias magnetic field close to a Feshbach resonance. It turns out that the physics of an unequal-population Fermi mixture in a trap is rather different from the uniform case. The dominant characteristic of the measured density profiles appears to be a phase separation, with an equal-density BCS phase in an interior core, and an outer shell consisting mostly of the majority species. If there are additional two-component phases, for instance Fulde-Ferrel-Larkin-Ovchinnikov (FFLO) phases, they are confined to a shell-shaped region between the outer majority shell and the inner BCS-like core.

Partridge et al. have reported in-situ measurements of the density profiles of the two states [4], while Zwierlein et al. report on measurements after expansion [5]. The former experiments are performed close enough to the Feshbach resonance that they may be regarded as being in the unitarity limit, i.e., in the limit that the interaction strength  $g$  is effectively infinite so it does not provide an energy scale to the problem. In this Letter we concentrate on the data from Ref. [4] and limit ourselves therefore to the unitarity region. We do not consider here the data of Ref. [5] on rotating fermion gases, nor do we deal with the issues arising from expansion after the trap is switched off.

We present a zero-temperature analysis of the phase separation using a local density approximation (LDA) and a BCS ansatz for the many-body wavefunction. The Feshbach resonance is treated using a single-channel de-

scription, because the closed-channel component of the Cooper pair wavefunctions is small in the crossover region for the extremely broad Feshbach resonance that is being used in the experiment [6, 7]. Based on an analysis of the uniform case at unitarity, we give simple arguments for the occurrence of phase separation, and to identify the surface that surrounds the BCS phase. We then calculate the majority and minority density profiles within the BCS ansatz, and compare with experimental profiles.

**BCS ansatz for the unitarity regime** | We first examine pairing at unitarity with unequal chemical potentials for a homogeneous mixture. Since we will treat the trapped case in LDA, the results from this analysis can be used locally for any point in the trap. We are interested in the  $g \rightarrow \infty$  limit of the Hamiltonian

$$\hat{H} = \sum_{\mathbf{k}; j} \epsilon_{\mathbf{k}; j} \hat{c}_{\mathbf{k}; j}^\dagger \hat{c}_{\mathbf{k}; j} + g \sum_{\mathbf{p}; \mathbf{q}; j} \hat{c}_{\mathbf{p}+\mathbf{k}; j}^\dagger \hat{c}_{\mathbf{q}}^\dagger \hat{c}_{\mathbf{k}; j} \hat{c}_{\mathbf{p}; j} :$$

The index  $j$  runs over the two hyperfine states of  $^6\text{Li}$ , denoted by  $|j\rangle$  and  $|\bar{j}\rangle$ . The masses are the same, so  $\epsilon_{\mathbf{k}} = \hbar^2 \mathbf{k}^2 / 2m$  for both species, but the chemical potentials are different, i.e.,  $\mu_{j, \bar{j}} \neq \mu$ , so that it is possible to have unequal densities  $n_{j, \bar{j}} \neq n$ .

We use the BCS wavefunction as an ansatz for the paired ground state. This corresponds to using the following decomposition for the interaction term:  $\sum_{\mathbf{k}} \hat{c}_{\mathbf{k}; j}^\dagger \hat{c}_{\mathbf{k}; j}^\dagger + \hat{c}_{\mathbf{k}; j} \hat{c}_{\mathbf{k}; j} = g$ . We restrict ourselves to zero-momentum pairing, because the experimental data do not indicate the presence of an FFLO state [8], and because two-channel calculations suggest that FFLO states are not stable close to the resonance [9]. At unitarity, the BCS ansatz is best understood as a variational approach as opposed to a mean-field approximation. For the case of an equal-density mixture, this approach has been shown to be a reasonable method of interpolating between the BCS and BEC limits. We employ the same philosophy here and extract information using the BCS expressions for the number density, energy density and the gap equation. Fortunately, improved information about the equal-density case is available from Monte-Carlo simulations [10, 11, 12] and may be used to improve our trap calculations.

For the equal-density case, and within the single-channel assumption, the many-body system at resonance is universal in the sense that the only energy scale in the problem is that set by the density, i.e., the Fermi energy of the corresponding free gas  $\mu_F$ . The BCS ansatz gives the energy of the resonantly interacting system to be  $0.59 \mu_F$ . This number is called  $1 + \lambda$ , with the universal number  $\lambda$  being known from Monte Carlo calculations to be  $\lambda \approx 0.58$  [10, 11, 12], to which the BCS value  $\lambda \approx 0.41$  should be regarded as an approximation. In the strong-coupling region, the pairing gap is of the order of the chemical potential, instead of being exponentially suppressed as in the weak-coupling regime. Within the BCS ansatz  $\mu_0 \approx 1.16 \mu_F$ , while Monte-Carlo calculations give  $\mu_0 \approx 0.84 \mu_F$  [12].

With differing chemical potentials, i.e.,  $\mu \neq 0$ , the quasiparticle spectrum of the BCS ansatz has two branches  $E_{k\pm} = E_k \pm \hbar\omega$ , with  $E_k = \sqrt{\mu^2 + \frac{\hbar^2 k^2}{2m}}$  [13]. For  $\mu > 0$ , the lower branch becomes negative in the momentum interval  $(k_1; k_2)$ , with  $k_{1,2} = \frac{\mu}{\hbar v_F}$ . In that case we need to fill up the negative energy modes to construct the lowest-energy ground state. As a result, the thermodynamic potential becomes

$$\Omega = \frac{1}{V} \sum_{\mathbf{k}} \left( \mu_{\mathbf{k}} E_{\mathbf{k}} + \frac{\hbar^2 k^2}{2m} - \frac{\hbar^2 k^2}{2m} \right) + \sum_{k_1 < k < k_2} \hbar\omega E_{\mathbf{k}}; \quad (1)$$

The  $\frac{\hbar^2 k^2}{2m}$  and  $-\frac{\hbar^2 k^2}{2m}$  terms are required to remove the usual ultraviolet divergence. Note that the last term is the only place where  $\hbar\omega$  enters. The gap equation is given by the condition for the extrema of the thermodynamic potential  $\frac{\partial \Omega}{\partial \hbar\omega} = 0$ . The density average and difference may be calculated as  $n = \frac{\partial \Omega}{\partial \mu}$  and  $m = \frac{\partial \Omega}{\partial \hbar\omega}$ . The resulting expressions also have contributions from the  $(k_1; k_2)$  shell in addition to the usual BCS contributions.

The ground state of the system is the absolute minimum of  $\Omega$ . For equal chemical potentials, the function  $\Omega(\mu; \hbar\omega)$  has a maximum at  $\hbar\omega = 0$  and a minimum at the equal-density gap  $\mu_0$ . As  $\hbar\omega$  is increased, there is a certain value,  $\hbar\omega = \mu_0 = \mu$ , at which the  $\hbar\omega = 0$  extremum becomes a minimum and there is an intermediate maximum. This maximum corresponds to an unequal-density paired solution of the gap equation, commonly known as the Samma phase [2], which is thus unstable. At some higher value of the chemical potential difference,  $\hbar\omega = \mu_0 = \mu$ , the  $\hbar\omega = 0$  solution becomes the global minimum so that the normal state is more stable than the paired state. For weak coupling ( $g \frac{1}{\mu} \ll 1$ ) the special values of  $\hbar\omega$  are  $\hbar\omega = \mu$  and  $\hbar\omega = \frac{\mu}{2}$ ,  $\mu_0 = 1.414 \mu$ . Moving towards the resonance from the BCS regime, we find that the values of  $\mu_1$  and  $\mu_2$  change only slightly within the BCS ansatz. The change in  $\mu_1$  is smaller than 1%, while we find that  $\mu_2$  evolves to about 1.44 at unitarity,

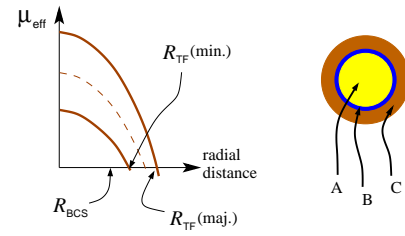


FIG. 1: Left: argument for phase separation from consideration of the local effective chemical potentials. Shown are  $\mu_{\text{eff}}(r)$  (dashed) and  $\mu_{\text{eff}}(r) + h$  (solid). Right: phase separation, after the  $x$  and  $y$  coordinates have been scaled to make the trap look spherically symmetric. Here A is the BCS core, C is the outer majority shell, B is the intermediate shell of bi-component phase which we treat as two non-interacting ideal gases.

i.e., a change of about 2%. The value of  $\mu_2$  at unitarity coupling is a universal number and our value  $\mu_2 = 1.44$  is the approximation to this universal number within the BCS ansatz.

Knowing that the Samma phase is a maximum of the thermodynamic potential in the uniform case, it is clear that we will not have this phase in the trap within the local-density approximation. Thus, barring more exotic pairing mechanisms, we only have to consider normal phases and equal-density BCS phases.

Phase separation in a trap | The trapping potential used in Ref. [4] is asymmetric and obeys  $V_{\text{trap}}(r) = \frac{1}{2} m \omega_z^2 z^2 + \frac{1}{2} m \omega_{\perp}^2 (x^2 + y^2)$ , with  $\omega_z = 2\pi \times 7.2$  Hz and  $\omega_{\perp} = 2\pi \times 350$  Hz. We scale the spatial variables in the radial directions so that the trap potential becomes spatially symmetric, with trapping frequency  $\omega_{\perp}$  in each direction. In LDA, the trap terms in the Hamiltonian are absorbed into the chemical potential, so that we have effective space-dependent chemical potentials:

$$\begin{aligned} \mu_e^{(1)}(r) &= \mu_1 - V_{\text{trap}}(r) = (\mu_1 + h) - \frac{1}{2} m \omega_z^2 z^2 \\ \mu_e^{(2)}(r) &= \mu_2 - V_{\text{trap}}(r) = (\mu_2 - h) - \frac{1}{2} m \omega_z^2 z^2 \end{aligned} \quad (2)$$

The average  $\mu_e = \frac{1}{2} (\mu_e^{(1)} + \mu_e^{(2)})$  decreases parabolically away from the center of the trap while the difference equals  $2h$  and stays constant. Near the center of the trap,  $h$  is small compared to  $\mu_e$  and hence compared to  $\mu_0(\mu_e)$ . Thus the densities are forced to be equal and we have a BCS phase in the center. Since  $\mu_e(r)$  decreases monotonically, there is some radius  $R_{\text{BCS}}$  at which  $\mu_0(\mu_e) \approx 1.16 \mu_e$  is equal to  $\mu_2 h$ . Outside this radius, a two-component normal phase is more stable than a superfluid state. For this phase, we ignore interactions between the two components and treat it like two ideal Fermi gases whose densities are determined by their different chemical potentials. At the Thomas-Fermi radius of the minority ( $\mu_2$ ) species,  $R_{\text{TF}}^{(2)} = \sqrt{\frac{2(\mu_2 - h)}{m \omega_z^2}}$ , the minority density vanishes.

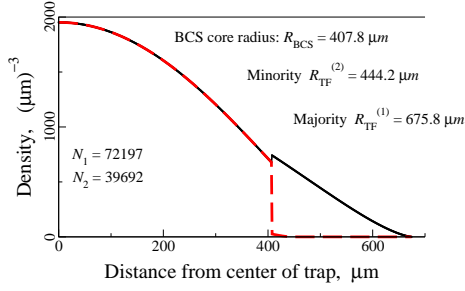


FIG. 2: Majority and minority densities calculated in LDA for typical experimental parameters of Ref. [4]. The densities are expressed in units for the effective spherical trap with trapping frequency  $\omega_z$  in each direction after rescaling the radial directions.

Outside  $r = R_{TF}^{(2)}$  only the majority remains. This outer shell survives up to the majority (Fermi) Thomas-Fermi radius  $R_{TF}^{(1)} = \frac{P}{2(\mu + \hbar)} = \frac{2}{\omega_z}$ .

Density profiles | Given the chemical potentials  $\mu$  at the trap center, we can calculate the BCS core radius  $R_{BCS}$  and the Thomas-Fermi radii  $R_{TF}^{(1;2)}$ . The densities are then given by

$$n_{1;2}(r) = \begin{cases} n_{BCS}(r) & r < R_{BCS} \\ n_N(\mu \pm \hbar) & R_{BCS} < r < R_{TF}^{(1;2)} \\ 0 & r > R_{TF}^{(1;2)} \end{cases} \quad (3)$$

Here  $n_{BCS}(r) = \frac{P}{(2\pi)^3} \int_{|\mathbf{k}| \leq E_k} d\mathbf{k} = 2V$  is the usual equal-density BCS density for a single component, and  $n_N(\mu) = (2\pi)^{-3} \int_{|\mathbf{k}| \leq \mu} d\mathbf{k} = \frac{2}{3} \mu^3$  is the ideal-gas density. At unitarity,  $n_{BCS}(\mu) = n_N(\mu) = \frac{2}{3} \mu^3$ . To calculate the density corresponding to given total atom numbers, we first find the chemical potentials which give  $N_{1;2} = \int n_{1;2}(r) dr$ , and then use the expressions given above.

In Fig. 2, we show density profiles for a typical experiment of Ref. [4]. Experimentally, the density itself is not accessible, but it is interesting to note some features. At the BCS core radius  $R_{BCS}$ , the majority density  $n_1(r)$  has a discontinuity because it is determined by the BCS density corresponding to  $\mu$  on the  $r < R_{BCS}$  side and by the normal density corresponding to  $\mu + \hbar$  on the  $r > R_{BCS}$  side. In the weak-coupling limit, the  $n_{BCS}(\mu)$  and  $n_N(\mu)$  functions are almost identical, and so the discontinuity would then have been much more prominent. At unitarity, however,  $n_{BCS}(\mu) = n_N(\mu) = \frac{2}{3} \mu^3$ , so that  $n_N(\mu) \approx 0.454 n_{BCS}(\mu)$  for our BCS treatment. This significantly reduces the upward jump of the majority density at the core edge.

Similarly, the minority density  $n_2(r)$  has a discontinuity at the BCS core edge as it jumps down from  $n_{BCS}(\mu)$  to  $n_N(\mu - \hbar)$ . This discontinuity is enhanced by the effect of nonzero  $\mu$  in  $n_N(\mu) = \frac{2}{3} (\mu + \hbar)^3 = 2 n_{BCS}(\mu)$ . The large decrease of the minority density assures that the minority Thomas-Fermi radius  $R_{TF}^{(2)}$  is only slightly larger than the

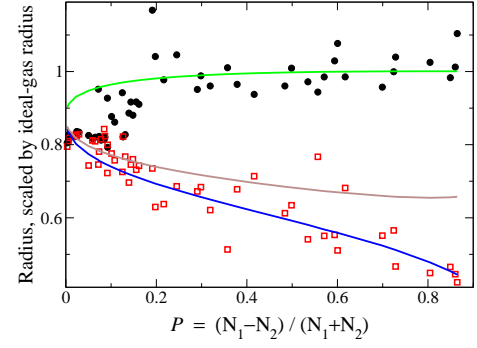


FIG. 3: Radius versus number asymmetry. The three solid lines from bottom to top are calculated values of  $R_{BCS}$ ,  $R_{TF}^{(2)}$  and  $R_{TF}^{(1)}$ . Filled circles and empty squares are experimental majority and minority radii from Ref. [4]. The radii  $R_{BCS}$ ,  $R_{TF}^{(2)}$  and the experimental minority radii are scaled by the ideal-gas Thomas-Fermi radius  $R_{TF}^{ideal}(N_2)$  of  $N_2$  (minority) fermions. The radius  $R_{TF}^{(1)}$  and the majority radii are scaled by  $R_{TF}^{ideal}(N_1)$ .

BCS core radius  $R_{BCS}$ , i.e., that the intermediate two-component shell is rather thin. In the real system, we expect the LDA discontinuities to be smoothed out somewhat by gradient and other corrections. Since experimentally only spatially integrated versions of  $n_1(r)$  (column densities) are observed, the small non-monotonicity of the majority density is further washed out and is expected to be difficult to observe.

Majority and minority radii | Fig. 3 shows the evolution of the three radii in our theory ( $R_{BCS}$ ,  $R_{TF}^{(2)}$ ,  $R_{TF}^{(1)}$ ) with the number asymmetry  $P = (N_1 - N_2) / (N_1 + N_2)$ , and compares with radii from Ref. [4]. Measured in units of the ideal-gas Thomas-Fermi radii corresponding to  $N_{1;2}$ , the theoretical curves depend only on  $P$  and not on the total number. The experimental radii are extracted by fitting the measured column density profiles to ideal-gas Thomas-Fermi distributions.

It is reasonable to assume that the experimental minority radii correspond to  $R_{BCS}$  rather than  $R_{TF}^{(2)}$ , since the minority occupancy in the intermediate shell is negligible, as shown in Fig. 2. Our *ab initio* LDA calculations then explain the radius data extremely well at large  $P$ . At small  $P$ , the calculated radii are somewhat higher than the experimental ones. This is expected from the use of the BCS ansatz, which underestimates the reduction of the paired state energy, and hence also the reduction of the size in a trap. We could improve our calculation by using the Monte Carlo values  $\mu_0 \approx 0.42 \mu_F$  and  $\mu_0 \approx 0.84 \mu_F$ . However, to identify  $R_{BCS}$  we also need the ratio  $\mu_0 = \mu_0 + \hbar$  at which the unequal-density normal phase becomes more stable than the equal-density paired phase, and to the best of our knowledge  $\mu_0$  is not known outside the BCS ansatz. We have therefore opted for consistency and used the BCS ansatz throughout.

The question remains whether there is a critical nonzero value of  $P$  at which phase separation first appears. No such feature appears in our calculations, because with the BCS treatment of unitarity, phase separation appears at any nonzero asymmetry, since only the equal-density BCS phase and the normal phase are stable in this case.

**Axial density profiles** | In Fig. 4, we have plotted LDA calculations for densities with both  $x$  and  $y$  directions integrated out, and compared them with column densities integrated along the  $x$  direction [8]. The typical feature seems to be that the majority density profile fits better than the minority profile, especially outside the BCS core. This is not so surprising because, outside the core, the majority distribution is simply the ideal-gas Thomas-Fermi distribution. Some details of the density profiles are smoothed out because of the double integration, but it is instructive to look at the axial density difference. In the integral for the axial density difference, one can for  $z < R_{\text{BCS}}$  remove  $z$  from both the integrand and the integration limits, so that the theoretical axial density difference is constant up to  $z = R_{\text{BCS}}$ , as seen in Fig. 4. In the experimental data, however, there is barely an extended constant part in the difference. Geometrically, the experimental data indicates that the inner core is expanded radially and squeezed axially compared to the LDA prediction. At this point the reason for this discrepancy is not clear. Possible reasons could be temperature effects, nonuniversal physics beyond the single-channel description, or the effects of nontrivial phases in the interface region which we have not included. Another intriguing possibility is that, since the trap is much tighter in the radial direction than in the axial direction, corrections to the local density approximation might be required for the radial directions. Chemical potentials are typically 5-15 times the energy corresponding to radial trapping frequency, the lower end of which might be near the limit of validity of LDA. The discrepancy in the density difference is an urgent issue and is presently under investigation.

**Conclusion** | In summary, we have presented ab initio calculations of the density profiles for a fermion mixture near a Feshbach resonance loaded into a trap and with unequal spin-populations. While the major features are successfully reproduced, two major questions emerge from our analysis. One is the shape of the axial density difference curve which deviates somewhat from the LDA calculation, as seen clearly in Fig. 4. The second issue is the possibility of having a transition from a non-phase-separated configuration to a phase-separated configuration at a certain critical value of the number asymmetry  $P$ .

We have assumed that unequal-density pairing schemes are less favored than the two-component normal phase of the intermediate shell. While it is likely that the intermediate shell is too small to make a difference

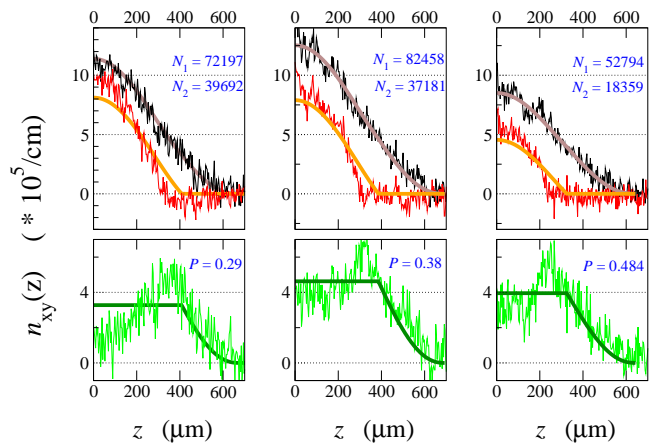


FIG. 4: Experimental axial densities as function of  $z$  for several  $(N_1; N_2)$ , plotted together with theoretical densities integrated over both  $x$  and  $y$  directions:  $\int dx dy n(x; y; z)$ . Upper panels are the axial densities of states  $|\downarrow\rangle$  and  $|\uparrow\rangle$  and the lower panels are the differences. Note that there are no fitting parameters.

in the density profiles, the issue of stability of various unequal-density pairing schemes has not been examined thoroughly at unitarity. Some of these questions and issues are currently also under investigation.

**Acknowledgments** | We thank Randy Hulet and Wen-hui Li for stimulating discussions and for providing experimental data. This work is supported by the Stichting voor Fundamenteel Onderzoek der Materie (FOM) and the Nederlandse Organisatie voor Wetenschappelijk Onderzoek (NWO).

Note: At the last stages of our work we learned of independent work discussing issues similar to ours [14, 15].

- 
- [1] P. Fulde and R. A. Ferrell, Phys. Rev. 135, A 550 (1964); A. I. Larkin and Y. N. Ovchinnikov, Zh. Eksp. Teor. Fiz. 47, 1136 (1964) [Sov. Phys. JETP 20, 762 (1965)].
  - [2] G. Samata, J. Phys. Chem. Solids 24, 1029 (1963).
  - [3] H. M. Uther and A. Sedrakian, Phys. Rev. Lett. 88, 252503 (2002); Phys. Rev. C 67, 015802 (2003).
  - [4] G. B. Partridge, W. Li, R. I. Kamar, Y. A. Liao, and R. G. Hulet, cond-mat/0511752. Published online in Science, Dec. 22, 2005.
  - [5] M. W. Zwierlein, A. Schirotzek, C. H. Schunck, and W. Ketterle, cond-mat/0511197. Published online in Science, Dec. 22, 2005.
  - [6] G. B. Partridge, K. E. Strecker, R. I. Kamar, M. W. Jack, and R. G. Hulet, Phys. Rev. Lett. 95, 020404 (2005).
  - [7] M. W. J. Romans and H. T. C. Stoof, Phys. Rev. Lett. 95, 260407 (2005).
  - [8] W. Li and R. G. Hulet, personal communication.
  - [9] D. E. Sheehy and L. Radzihovsky cond-mat/0508430.
  - [10] J. Carlson, S. Y. Chang, V. R. Pandharipande, and K. E. Schmidt, Phys. Rev. Lett. 91, 050401 (2003).

- [1] G. E. Astrakharchik, J. Boronat, J. Casulleras, and S. Giorgini, Phys. Rev. Lett. 93, 200404 (2004).
- [2] J. Carlson and S. Reddy, Phys. Rev. Lett. 95, 060401 (2005).
- [3] M. Houbiers, R. Ferwerda, H. T. C. Stoof, W. I. McAlexander, C. A. Sackett, and R. G. Hulet, Phys. Rev. A 56, 4864 (1997).
- [4] W. Yi and L.-M. Duan, cond-mat/0601006.
- [5] F. Chevy, cond-mat/0601122.